Two-region semi-analytical solution for latent heat thermal energy storage systems

Mojtaba Safdari[1], Sadegh Sadeghzadeh[*2], Rouhollah Ahmadi[3], Fatemeh Molaei[4]

1- MSc of Energy department, School of Advanced Technologies, Iran University of Science and Technology, Tehran, Iran, mojtaba.safdari.mm@gmail.com
2- Associate Professor, Nanotechnology department, School of Advanced Technologies, Iran University of Science and technology, Tehran, Iran, sadeghzadeh@iust.ac.ir
3- Associate Professor, Energy department, School of Advanced Technologies, Iran University of Science and technology, Tehran, Iran, ahmadi@iust.ac.ir
4- Ph.D. student, Mining and Geological Engineering Department, The University of Arizona, Arizona, USA

ABSTRACT

Problems with Latent Heat Thermal Storage (LHTS) often contain several boundary conditions that an exact solution cannot solve. Therefore novel methods to tackle such issues could fundamentally change the design of innovative energy storage systems. This study concentrates on the reformulation of the Generalized Differential Quadrature Method (GDQM) for the two-region freezing/melting Stefan problem as an essential LHTS challenge. Comparison and convergence show that there is sufficient confidence in the proposed approach. By monitoring the precision of the suggested approach for the LHTS problem, it was indicated that this method's error depends on Stefan's number. The maximum error of all Stefan numbers up to 0.3 is less than 6 %. For such applications in a standard array of LHTS (Stefan numbers between 0-0.2), The proposed method is appropriate as it predicts the answers with a maximum of 4.2% error. In

* Corresponding author (sadeghzadeh@iust.ac.ir)

comparison to the heat capacity method, GDQM delivers a more precise result at higher processing times. Additionally, this GDQM priority is accompanied by a low computational cost, which is unquestionably superior.

Keywords: Generalized Differential Quadrature Method (GDQM); Two-region Stefan problem; Thermal Storage (TS); Solidification; Phase Change Materials (PCM); Melting

NOMENCLATURE

$T_1(x,t)$	liquid temperature, K	W_I	interior temperature Vector
$T_2(x,t)$	solid temperature, K	W_B	boundary temperature vector
$T_l(\theta_l), T_0$	left front temperature, K	$\dot{W}_I$	temperature's derivative vector
$T_m(\theta_m)$	transition temperature, K	$\dot{S}$	interface location derivative
$T_r(\theta_r)$	right front temperature, K	A,G	weight coefficients matrix
$T_i(\theta_i)$	initiate temperature, K	I	identity matrix
T_∞	ambient temperature	Ω	scalar
s(t)/S	location of the interface, m	Subscript	
t(s)/(τ)	time, s	i	initial condition
h	Fusion enthalpy, W/(m^2.K)	l/r	Left/right
L	length of the reference, m	m	melting
N/M	Node's number, liquid/solid	I	interior
h_{sl}	latent heat of melting, kJ/kg	B	boundary
C_p	specific heat, kJ/(kg.K)	BC	boundary condition
ρ	density, kg/m^3	EX	exact
α	thermal diffusivity, m^2/s	1	liquid
k	thermal conductivity, W/(m.K)	2	solid
n	order of derivative		
Ste	Stefan number	Superscript	
q_0'', q	heat flux, $W/(m^2K)$	1,2	1st and 2nd degree of GDQ

1 Introduction

Various methods such as enthalpy [1], heat capacity [2], and integral method [3, 4] have been employed to solve the problems with melting/solidification. On the other side, many types of discrete methods, for example, finite element (FEM) [5-7], finite volume (FVM) [8], and finite difference (FDM) [9] were implemented.

These techniques facilitate the design requirements in complex questions, but the precision and computational expenses are still arguable. It will revolutionize PCM-based LHTS systems' design if there would be a precise and computationally effective numerical approach that can solve LHTS problems with arbitrary boundary conditions. The differential quadrature method (DQM) is addressed as the most robust choice with such functionalities with a limited required node to achieve a semi-exact reaction and impressive precision [10].

GDQM varies from FEM in two attributes; Firstly, the finite element method utilizes low-order polynomials to estimate an equation at the level of a local element. At the same time, GDQ uses higher-order polynomials to estimated a function across the entire area. Secondly, in GDQM, derivatives of a function are being quantified directly over a node. In contrast, the finite element method moves toward a function on a single limited node, which could be concluded from an estimated function. DQM was expressed by Bellman et al. [11, 12] as the principal formula of GDQM to solve partial differential equations.

To discretize partial derivatives, the primary challenge of DQM is the requirement for coefficient weighting. Bellman et al. [12] introduced two main discretization methods. For whole polynomials with a order smaller or equivalent to N-1, the first is the resolution of a number of linear algebraic equations which satisfy the linear constrained relationship, that N denotes the inclusive nodes inside the discretized region. A series of N-N linear algebraic equations should be determined for any order of derivative in this approach.

The second method uses roots for grid nodes in an Nth degree shifted Legendre polynomial to compute weighting coefficient using an algebraic formula. So, for every single N value and all problems and boundary conditions, the node position is fixed in the grid. In some problems, it is evident that the answer requires several additional nodes nearby a certain node to improve the answer's precision. Both methods are, therefore, a challenge to implement. To overcome these limitations,

Shu & Richard [13, 14] developed a generalized differential quadrature (GDQ), which was specifically established to explain fluid mechanics problems [15]. This method substitutes a factored linear summation of the entire function's local values at each node with a weighted linear summation in a partial derivative grid. This approach deals with all PDE in various applications [16-21]. It has not yet been used to solve LHTS problems, despite the significant capabilities of this method.

This method is used in many models and system optimizations applications, including free vibration analysis [22, 23], mixed static and dynamic structural response [24, 25], CFD [26, 27], Burgers' equations [28], waveguide examination [29], equation of Helmholtz [30], transportation notions and diffusion [19], etc. Scientists have used this approach to solve heat transfer problems as the most relevant case for LHTS. Shu used the GDQM in a square cavity to mimic natural convection [31]. The findings found that both the precision and the convergence rate can be improved by this method. To calculate heat conductivity over a one-dimensional plate, Ming et al. employed DQM to the reverse heat conduction matter [32]. Tomasiello et al. proposed an explicit arrangement for the numeral approach for one-dimensional non-linear heat transfer in the domain of zone-time employing quadrature regulations. [33]. Another researcher resolved non-linear heat as well as mass transmission equations in one and two dimensions [34].

Malekzadeh established a differential quadrature element (DQEM) technique concerning the non-linear, transitory thermal conduction study of expanded sides [35]. This research described spatial domains as subdomains and called every subdomain as an element. Convection-radiation heat transfer circumstances and whole domain areas were taken into account. Several lab works containing diverse degrees of complexity in geometry and loading have been considered for convergence, precision, and numerical solidity of the findings.

In other articles [36, 37], the authors of this article solved the Stefan problem, which deals with the problem of phase change as one region, using this method

(GDQ). The results showed that using this method to solve the issues of phase change material (PCM) can quickly and accurately predict these materials' behavior. In solving one region problem, the temperature profile is checked only in the liquid part. However, the preliminary temperature is different from the phase change temperature in real conditions. In this case, the problem becomes two-region, and the temperature profile in the solid part must also be examined. Therefore, in this paper, the changing phase of phase change materials using the GDQ method in two-region mode has been investigated. The comparisons demonstrate that using a mapping technique and later inverting the resolved question, the GDQM method applies to two-region PCM-based problems with excellent precision and steadiness.

2 Fundamentals of Generalized differential quadrature method (GDQM) for Stefan Problem

Solid-liquid interphase moves alongside the medium through phase change materials' melting/solidification process (PCM). The problem's name is the Stefan problem, which can move an outer limit like other probable applications. Stefan's situation for a PDE is a specific type of problem with boundary value thermal conduction. This problem primarily categorizes into two parts: one-region as well as two-region problems. Provided that $T_i = T_m$ (T_i is the preliminary and T_m is the liquefying temp.) the temperature distribution in the solid region remains constant over the phase changing procedure. In these circumstances, only in the liquid region the temperature distribution is unknown and must be obtained, and the Stefan problem will be recognized as the one-region problem. however, if the initial temperature falls below the phase change temperature, then the thermal equations of the liquid phase as well as the solid phase must be solved.; the meaning of the two-region Stefan problem [38].

Figure 1 illustrates the physical scheme of the two-region melting issue.

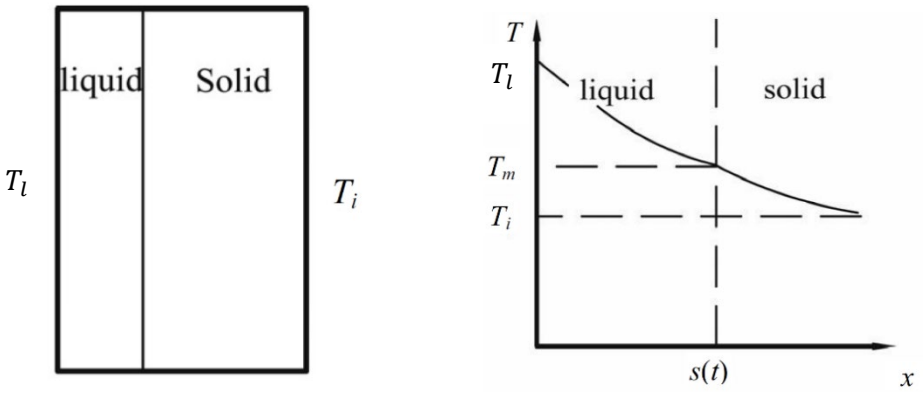

Figure 1. conduction controlled melting (left) and two-region melting problem (right) [38]

The uncertainty in the solid-liquid interface position results in an exclusive complexity in solidification/melting problems. Since the boundary changes constantly, the related problems are defined as problems with the moving boundary, and time is an independent parameter permanently. In this simulation, natural convection is ignored, and the heat transfer mechanism is pure heat conduction. This is referred to as a conduction control model in this context. Therefore, the following assumptions should be considered to solve these questions as shown in Figure 1. [39]:

- s(t) is with no thickness.
- T_m at the interface is constant and identified
- h_{sl}, c_p, and k are constant.
- There is no change in volume during phase change
- Nucleation and subcooling are ignored
- PCM's density does not change in the solid or liquid phase
- In the liquid phase, natural convection is ignored, and pure conduction is the heat transfer mechanism in both phases.

3 Mathematical model

3.1 Two-region phase change problem

The phase transition issue studied here is schematically shown in figure 1, where $T_i = T_m$. The temperature distribution in the solid region remains unchanged at the melting temperature. When $T_i < T_m$, the melting or solidification concern develops a two-region problem, so the liquid and solid region's temperature distribution is unknown. At time $t = 0$, the temperature at the boundary $x = 0$ (left wall of the finite slab), is unexpectedly augmented to a temperature $T_l > T_m$ and also the temperature of the $x = L$ (right side of the finite slab) reaches up to $T_r = T_i < T_m$ in the same way.

The primary indeterminacies with investigating the PCMs are to define the location of the moving interphase $s(t)$, the temperature distribution in the liquid zone $T_1(x,t)$ and in the solid region $T_2(x,t)$. In general, the leading equation in liquid and solid mediums to find an answer for a melting problem should be the following equations [38]:

$$(T_1)_{xx} = 1/\alpha_1.(T_1)_t \qquad 0 < x < s(t) \qquad t > 0 \qquad (1)$$
$$T_1(x,t) = T_l \qquad x = 0 \qquad t > 0 \qquad (2)$$
$$(T_2)_{xx} = 1/\alpha_2.(T_2)_t \qquad s(t) < x < L \qquad t > 0 \qquad (3)$$
$$T_2(x,t) = T_r = T_i \qquad x = L \qquad t > 0 \qquad (4)$$
$$T_1(x,t) = T_2(x,t) = T_i \qquad x > 0 \qquad t = 0 \qquad (5)$$

These equations are linked with subsequent interface energy-balance mathematical statements at the boundary face:

$$T_1(x,t) = T_2(x,t) = T_m \qquad x = s(t),\ t > 0 \qquad (6)$$

$$k_1(T_1)_x - k_2(T_2)_x = \rho.h_{sl}.\dot{s}(t) \qquad (7)$$

Where $\alpha(m^2.s^{-1})$, $\rho(kg.m^{-3})$, $k(W.m^{-1}K^{-1})$, $h_{sl}(kJ/kg)$ and $s(t)$ indicate the thermal diffusivity, density, conductivity, latent heat, and interphase location, respectively.

3.2 Non-dimensionalized structure of the Equations

Using the GDQ method requires that the equations be non-dimensionalized. Introducing the following dimensionless variables, equations (1) to (7) were reformulated [38]:

$$\theta = \frac{T_m - T}{T_m - T_l},\ \theta_i = \frac{T_m - T_i}{T_m - T_l},\ X = \frac{x}{L},\ S = \frac{s}{L},\ \tau = \frac{\alpha t}{L^2},\ Ste = \frac{c_{p_1}(T_m - T_0)}{h_{sl}} \quad (8)$$

L denotes a specific length of the problem and can be calculated by the nature of it, which is equal to the ice/liquid slab's length in this paper. The dimensionless mathematical formulations for the two-region problem are as follows: [38]:

$$(\theta_1)_{XX} = (\theta_1)_\tau \qquad 0 < X < S \qquad \tau > 0 \quad (9)$$
$$Na.(\theta_2)_{XX} = (\theta_2)_\tau \qquad S(\tau) < X < 1 \qquad \tau > 0 \quad (10)$$
$$(\theta_1)_X - Nk.(\theta_2)_X = Ste^{-1}\dot{S} \qquad X = S \qquad \tau > 0 \quad (11)$$
$$\theta(0,\tau) = \theta_l \quad (12)$$
$$\theta(1,\tau) = \theta_r \quad (13)$$
$$\theta(S,\tau) = \theta_m \quad (14)$$
$$\theta(X,0) = \theta_i \quad (15)$$

Where $Na = a_2 a_1^{-1},\ and\ Nk = k_2 k_1^{-1}$.

Using the front-fix transformation and describing the new dimensionless variable of y and z as follows:

$$y = X.S^{-1} \quad (16)$$
$$z = (X - S).(1 - S)^{-1} \quad (17)$$

Equations (9) – (15) are time-dependent, and their non-dimensionalized form is reported below:

$$S^{-2}(\theta_1)_{yy} + y.S^{-1}.\dot{S}.(\theta_1)_y = (\theta_1)_\tau \qquad 0 < y < 1 \qquad \tau > 0 \quad (18)$$
$$Na.(1 - S)^{-2}.(\theta_2)_{zz} + (1 - z).(1 - S)^{-1}.\dot{S}.(\theta_2)_z = (\theta_2)_\tau \qquad 0 < z < 1 \qquad \tau > 0 \quad (19)$$
$$S^{-1}(\theta_1)_y - Nk.(1 - S)^{-1}.(\theta_2)_z = Ste^{-1}\dot{S} \qquad X = S \qquad \tau > 0 \quad (20)$$
$$\theta_1(0,\tau) = \theta_l \quad (21)$$
$$\theta_2(1,\tau) = \theta_r \quad (22)$$
$$\theta_1(1,\tau) = \theta_2(0,\tau) = \theta_m \quad (23)$$
$$\theta_1(y,0) = \theta_2(z,0) = \theta_i \quad (24)$$

The GDQM is more stable with this exchange because the problem was transformed to the [0 1] space [38].

4 Solution Approach

4.1 GDQM

A more reliable and steady approach that accomplishes the boundary conditions and produces precise and stable results with only a few grid points has recently been developed. The generalized differential quadrature method (GDQM) was developed for this approach, especially in the melting/solidification question. In principle, the GDQM can be applied to switch derivatives in a discrete point with a total of several weighted functions.

$$\frac{\partial^n f(x,z)}{\partial x^n}\Big|_{x=X_i} = \sum_{j=1}^{N} {c_{ij}}^n f(x_j,z) \qquad (i = 1,2,\dots,N) \tag{25}$$

Where, $x_i, n, N, f, X_i and$ c_{ij} indicate the coordinates, derivative order, sum of discrete points, specified function, nodes in the direction of x_i that their derivative is required, and the factors (at point X_i, n^{th} order of derivative, x_i direction), respectively. A recursive formula is established to calculate the weight factors as follows: [40]:

$$\begin{cases} {c_{ij}}^{(n)} = n\left[a_{ij}c_{ii}^{(n-1)} - \dfrac{c_{ij}^{(n-1)}}{x_i - x_j}\right] & (i \neq j \text{ و } i,j = 1{:}\,N;\ \ n = 2{:}\,N-1) \\ {c_{ii}}^{(n)} = -\sum_{j=1,j\neq i}^{N} {c_{ij}}^{(n)} & \left(i = j \text{ و } i,j = 1{:}\,N\right) \end{cases} \tag{26}$$

where a_{ii} and $a_{ij}$are the first derivative coefficients and are calculated by [40]:

$$\begin{cases} a_{ij} = \dfrac{M^{(1)}(x_i)}{(x_i - x_j).M^{(1)}(x_j)} & (i \neq j) \\ a_{ii} = -\sum_{j=1,j\neq i}^{N} a_{ij} & (i = j) \end{cases} \tag{27}$$

Where

$$M^{(1)}(x_i) = \prod_{k=1,k\neq i}^{N} (x_i - x_k) \quad (28)$$

The sampling points are used as numerical computations with the approach of Chebyshev-Gauss-Lobatto

$$x_i = \frac{L}{2}\left(1 - cos\frac{i-1}{N-1}\pi\right), \qquad i = 1,2,\dots,N \quad (29)$$

The length of the considered path is denoted by the letter L. This method can be utilized to discretize the equations of motion and also boundary conditions. Then, an algebraic set of equations can be determined by transforming the problem equations into GDQ form.

4.2 Transformation to GDQ euations

Two-region melting/solidification formulations are given by the equations (18) to (24). As shown in figure 1, the left, initial, and right sides of the slab have a constant temperature in these equations. As in figure 2, the first and last nodes are supposed to be boundary nodes in $0 < y < 1$ and $0 < z < 1$ domain, and $i = 2$ to $N - 1$ (liquid region) and $j = 2$ to $M - 1$ (solid region) as internal nodes. Discretizing the introduced transformed formulation, the heat transfer equations (18) and (19) is rewritten in the shape of vector as:

$$S^{-2}(\mathrm{A_{IB}}^{(2)}\mathrm{W_B} + \mathrm{A_{II}}^{(2)}\mathrm{W_I})_1 + yS^{-1}\dot{S}\left(\mathrm{A_{IB}}^{(1)}\mathrm{W_B} + \mathrm{A_{II}}^{(1)}\mathrm{W_I}\right)_1 = (\dot{\mathrm{W}}_\mathrm{I})_1 \quad (30)$$

$$Na.(1-S)^{-2}.(\mathrm{A_{IB}}^{(2)}\mathrm{W_B} + \mathrm{A_{II}}^{(2)}\mathrm{W_I})_2 + (1-z).(1-S)^{-1}.\dot{S}.\left(\mathrm{A_{IB}}^{(1)}\mathrm{W_B} + \mathrm{A_{II}}^{(1)}\mathrm{W_I}\right)_2 = (\dot{\mathrm{W}}_\mathrm{I})_2 \quad (31)$$

Where $\mathrm{W_B}$ and $\mathrm{W_I}$ are both internal and boundary values. $\mathrm{A_{IB}}$and $\mathrm{A_{II}}$ are coefficient matrices that correspond to the boundary temperature and internal temperature coefficients in internal equations. Additionally, the time derivative of the internal temperatures is $\dot{\mathrm{W}}_\mathrm{I}$.

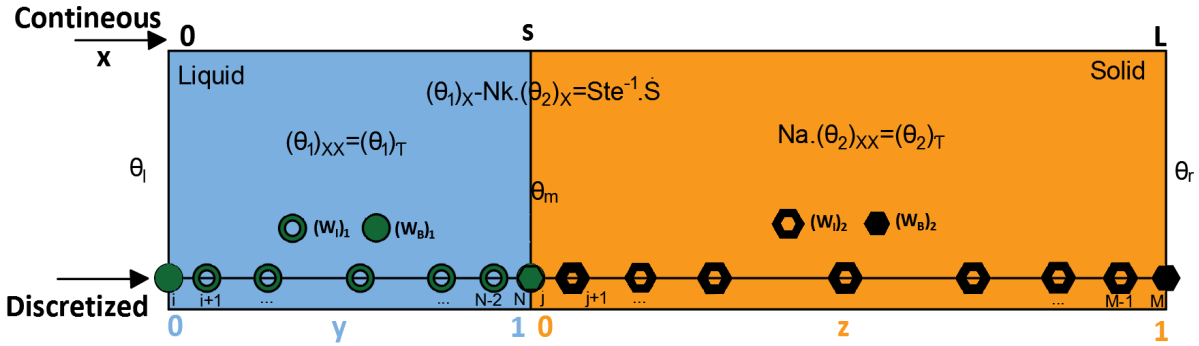

Figure 2. The continuous and GDQ-based discretized zones are represented using imposed governing equations.

The primary equation is linked to the Stefan boundary condition given by Eq. (20) in the two-region issue. The discretized form of the equations is shown below:

$$S^{-1}\left(\mathrm{G}_{\mathrm{BB}}^{(1)}\mathrm{W}_{\mathrm{B}}+\mathrm{G}_{\mathrm{BI}}^{(1)}\mathrm{W}_{\mathrm{I}}\right)_1-Nk.(1-S)^{-1}.\left(\mathrm{G}_{\mathrm{BB}}^{(1)}\mathrm{W}_{\mathrm{B}}+\mathrm{G}_{\mathrm{BI}}^{(1)}\mathrm{W}_{\mathrm{I}}\right)_2=\Omega_B\,\dot{S} \quad (32)$$

Where $\mathrm{G}_{\mathrm{BI}},\mathrm{G}_{\mathrm{BB}}$ represent the factors of boundary and interior temperatures correspondingly of boundary conditions and Ω_B denotes a constant (-1/Ste). The boundary conditions can be ordered using equations (21) and (23) as follows:

$$(\mathrm{A}_{\mathrm{BB}}\mathrm{W}_{\mathrm{B}})_1=(\theta_{\mathrm{BC}})_1 \quad (33)$$

$$(\mathrm{A}_{\mathrm{BB}}\mathrm{W}_{\mathrm{B}})_2=(\theta_{\mathrm{BC}})_2 \quad (34)$$

Where A_{BB} is a 2×2 identity matrix, $(\theta_{\mathrm{BC}})_1=[\theta_{\mathrm{l}}\;\theta_{\mathrm{m}}]^T$ and $(\theta_{\mathrm{BC}})_2=[\theta_{\mathrm{m}}\;\theta_{\mathrm{r}}]^T$. Equations (30) to (32) can be combined as a rough replacement:

$$S^{-2}(\mathrm{A}_{\mathrm{IB}}{}^{(2)}\theta_{\mathrm{BC}}+\mathrm{A}_{\mathrm{II}}{}^{(2)}\mathrm{W}_{\mathrm{I}})_1+yS^{-1}\dot{S}\left(\mathrm{A}_{\mathrm{IB}}{}^{(1)}\theta_{\mathrm{BC}}+\mathrm{A}_{\mathrm{II}}{}^{(1)}\mathrm{W}_{\mathrm{I}}\right)_1=(\dot{\mathrm{W}}_{\mathrm{I}})_1 \quad (35)$$

$$Na.(1-S)^{-2}.(\mathrm{A}_{\mathrm{IB}}{}^{(2)}\theta_{\mathrm{BC}}+\mathrm{A}_{\mathrm{II}}{}^{(2)}\mathrm{W}_{\mathrm{I}})_2+(1-z).(1-S)^{-1}.\dot{S}.\left(\mathrm{A}_{\mathrm{IB}}{}^{(1)}\theta_{\mathrm{BC}}+\mathrm{A}_{\mathrm{II}}{}^{(1)}\mathrm{W}_{\mathrm{I}}\right)_2=(\dot{\mathrm{W}}_{\mathrm{I}})_2 \quad (36)$$

$$\Omega_B^{-1}(S^{-1}\left(\mathrm{G}_{\mathrm{BB}}^{(1)}\theta_{\mathrm{BC}}+\mathrm{G}_{\mathrm{BI}}^{(1)}\mathrm{W}_{\mathrm{I}}\right)_1-Nk.(1-S)^{-1}.\left(\mathrm{G}_{\mathrm{BB}}^{(1)}\theta_{\mathrm{BC}}+\mathrm{G}_{\mathrm{BI}}^{(1)}\mathrm{W}_{\mathrm{I}}\right)_2)=\dot{S} \quad (37)$$

This arrangement is entirely adjustable to the state-space format. Now a promising typical state-space arrangement is obtained as below;

$$\frac{\mathrm{d}}{\mathrm{d}\tau}\{\mathrm{W_I}\}_1 = \left(\left[S^{-2}\mathrm{A_{II}}^{(2)} + yS^{-1}\dot{S}\mathrm{A_{II}}^{(1)}\right]\{\mathrm{W_I}\}\right)_1 + \\ + \left(\left[S^{-2}\mathrm{A_{IB}}^{(2)} + yS^{-1}\dot{S}\mathrm{A_{IB}}^{(1)}\right]\{\theta_{\mathrm{BC}}\}\right)_1 \quad (38)$$

$$\frac{\mathrm{d}}{\mathrm{d}\tau}\{\mathrm{W_I}\}_2 = \left(\left[Na.(1-S)^{-2}\mathrm{A_{II}}^{(2)} + (1-z)(1-S)^{-1}\dot{S}\mathrm{A_{II}}^{(1)}\right]\{\mathrm{W_I}\}\right)_2 + \\ + \left(\left[Na.(1-S)^{-2}\mathrm{A_{IB}}^{(2)} + (1-z).(1-S)^{-1}\dot{S}\mathrm{A_{IB}}^{(1)}\right]\{\theta_{\mathrm{BC}}\}\right)_2 \quad (39)$$

$$\frac{\mathrm{d}}{\mathrm{d}\tau}\{\dot{S}\} = \Omega_B^{-1}\left(\left[\mathrm{G_{BI}}^{(1)}S^{-1}\right]\{\mathrm{W_I}\}\right)_1 - \left(\left[\mathrm{G_{BI}}^{(1)}Nk(1-S)^{-1}\right]\{\mathrm{W_I}\}\right)_2 + \left(\left[S^{-1}\mathrm{G_{BB}}^{(1)}\right]\{\theta_{\mathrm{BC}}\}\right)_1 \\ - \left(\left[Nk(1-S)^{-1}\mathrm{G_{BB}}^{(1)}\right]\{\theta_{\mathrm{BC}}\}\right)_2 \quad (40)$$

To acquire a set of algebraic equations, equations (38) to (40) should now be practical to all interior nodes i= 2,3,...,N-1. Numerical simulation is carried out using the fourth-order method of Runge Kutta as it is the most popular method of integration in state-space models over time. The offered methodology is a particular instance of the Stefan problem, and it is possible to study different case studies for real conditions. Several potential problems are listed in table 1.

Table 1. Equations, constitutive relationship, as well as techniques for solving different issues including Stefan problem

Problem and boundary condition Condition			**Solution approach**
	Static (temperature)	**Static (heat flux)**	**Algebraic**
Equation	$\begin{cases} (A_{IB}{}^{(2)}\theta_{BC} + A_{II}{}^{(2)}W_I)_1 = 0 \\ \left(\mathrm{A_{IB}}{}^{(2)}\theta_{\mathrm{BC}} + \mathrm{A_{II}}{}^{(2)}\mathrm{W_I}\right)_2 = 0 \\ (\mathrm{A_{BB}W_B})_{1\&2} = (\theta_{\mathrm{BC}})_{1\&2}, \mathrm{A_{BB}} = I \end{cases}$	$\begin{cases} (A_{IB}{}^{(2)}\theta_{BC} + A_{II}{}^{(2)}W_I)_1 = 0 \\ \left(\mathrm{A_{IB}}{}^{(2)}\theta_{\mathrm{BC}} + \mathrm{A_{II}}{}^{(2)}\mathrm{W_I}\right)_2 = 0 \\ (\mathrm{A_{BB}}{}^{(1)}\mathrm{W_B} + \mathrm{A_{BI}}{}^{(1)}\mathrm{W_I})_1 = \mathrm{Q_{BC}} \\ (\mathrm{A_{BB}W_B})_2 = (\theta_{\mathrm{BC}})_2, \mathrm{A_{BB}} = I \end{cases}$	
Constitutive relation	$\begin{cases} (\mathrm{W_I})_1 = -(A_{II}^{-1(2)}A_{IB}{}^{(2)}\theta_{BC})_1 \\ (\mathrm{W_I})_2 = -(A_{II}^{-1(2)}A_{IB}{}^{(2)}\theta_{BC})_2 \\ \mathrm{W_B} = \theta_{\mathrm{BC}} \end{cases}$	$\begin{cases} W_I = \left(A_{IB}{}^{(2)}\mathrm{A_{BB}^{-1}}{}^{(1)}\mathrm{A_{BI}}{}^{(1)} - A_{II}{}^{(2)}\right)^{-1}(A_{IB}{}^{(2)}A_{BB}^{-1(1)}Q_{BC}) \\ (\mathrm{W_I})_2 = -(A_{II}^{-1(2)}A_{IB}{}^{(2)}\theta_{BC})_2 \\ (\mathrm{W_B})_2 = (\theta_{\mathrm{BC}})_2 \end{cases}$	
Dynamic (temperature)			**Runge-Kutta**
Equation	$\begin{cases} S^{-2}\left(A_{IB}{}^{(2)}W_B + A_{II}{}^{(2)}W_I\right)_1 + yS^{-1}\dot{S}\left(A_{IB}{}^{(1)}W_B + A_{II}{}^{(1)}W_I\right)_1 = (\dot{W}_I)_1 \\ Na.(1-S)^{-2}.(A_{IB}{}^{(2)}W_B + A_{II}{}^{(2)}W_I)_2 + (1-z).(1-S)^{-1}.\dot{S}.\left(A_{IB}{}^{(1)}W_B + A_{II}{}^{(1)}W_I\right)_2 = (\dot{W}_I)_2 \\ S^{-1}\left(G_{BB}^{(1)}W_B + G_{BI}^{(1)}W_I\right)_1 - Nk.(1-S)^{-1}.\left(G_{BB}^{(1)}W_B + G_{BI}^{(1)}W_I\right)_2 = \Omega_B\dot{S} \\ (\mathrm{A_{BB}W_B})_{1\&2} = (\theta_{\mathrm{BC}})_{1\&2}, \mathrm{A_{BB}} = I \end{cases}$		
Constitutive relation	$\begin{cases} \frac{\mathrm{d}}{\mathrm{d}\tau}\{\mathrm{W_I}\}_1 = ([S^{-2}\mathrm{A_{II}}{}^{(2)} + yS^{-1}\dot{S}\mathrm{A_{II}}{}^{(1)}]\{\mathrm{W_I}\})_1 + ([S^{-2}\mathrm{A_{IB}}{}^{(2)} + yS^{-1}\dot{S}\mathrm{A_{IB}}{}^{(1)}]\{\theta_{\mathrm{BC}}\})_1 \\ \frac{\mathrm{d}}{\mathrm{d}\tau}\{\mathrm{W_I}\}_2 = \left([Na.(1-S)^{-2}\mathrm{A_{II}}{}^{(2)} + (1-z)(1-S)^{-1}\dot{S}\mathrm{A_{II}}{}^{(1)}]\{\mathrm{W_I}\}\right)_2 \\ + \left([Na.(1-S)^{-2}\mathrm{A_{IB}}{}^{(2)} + (1-z).(1-S)^{-1}\dot{S}\mathrm{A_{IB}}{}^{(1)}]\{\theta_{\mathrm{BC}}\}\right)_2 \\ \frac{\mathrm{d}}{\mathrm{d}\tau}\{\dot{S}\} = \Omega_B^{-1}\left([\mathrm{G_{BI}}{}^{(1)}S^{-1}]\{\mathrm{W_I}\}\right)_1 - \left([\mathrm{G_{BI}}{}^{(1)}Nk(1-S)^{-1}]\{\mathrm{W_I}\}\right)_2 + \left([S^{-1}\mathrm{G_{BB}}{}^{(1)}]\{\theta_{\mathrm{BC}}\}\right) - \left([Nk(1-S)^{-1}\mathrm{G_{BB}}{}^{(1)}]\{\theta_{\mathrm{BC}}\}\right)_2{}_1 \\ (\mathrm{A_{BB}W_B})_{1\&2} = (\theta_{\mathrm{BC}})_{1\&2}, \mathrm{A_{BB}} = I \end{cases}$		
Dynamic (heat flux at boundaries)			**Runge-Kutta**
Equation	$\begin{cases} S^{-2}\left(A_{IB}{}^{(2)}W_B + A_{II}{}^{(2)}W_I\right)_1 + yS^{-1}\dot{S}\left(A_{IB}{}^{(1)}W_B + A_{II}{}^{(1)}W_I\right)_1 = (\dot{W}_I)_1 \\ Na.(1-S)^{-2}.(A_{IB}{}^{(2)}W_B + A_{II}{}^{(2)}W_I)_2 + (1-z).(1-S)^{-1}.\dot{S}.\left(A_{IB}{}^{(1)}W_B + A_{II}{}^{(1)}W_I\right)_2 = (\dot{W}_I)_2 \\ S^{-1}\left(G_{BB}^{(1)}W_B + G_{BI}^{(1)}W_I\right)_1 - Nk.(1-S)^{-1}.\left(G_{BB}^{(1)}W_B + G_{BI}^{(1)}W_I\right)_2 = \Omega_B\dot{S} \\ S^{-1}\Omega_{BB}{}^{-1}\left(\mathrm{A_{BB}}{}^{(1)}\mathrm{W_B} + \mathrm{A_{BI}}{}^{(1)}\mathrm{W_I}\right)_1 = \mathrm{Q_{BC}} \\ \text{Constant heat flux(Neumann condition):} \\ \mathrm{Q_{BC}} = Scalar \\ Natural\ convection: \\ \mathrm{Q_{BC}} = (\mathrm{T_\infty} - \mathrm{T_m})\left(\frac{s}{k} + \frac{1}{h}\right) = \Omega_{BB1}S + \Omega_{BB2} \end{cases}$		
Constitutive relation	$\begin{cases} \frac{\mathrm{d}}{\mathrm{d}\tau}\{\mathrm{W_I}\}_1 = \left(\left[S^{-2}\mathrm{A_{II}}{}^{(2)} - S^{-2}A_{IB}{}^{(2)}\mathrm{A_{BB}^{-1}}{}^{(1)}\mathrm{A_{BI}}{}^{(1)} - yS^{-1}\dot{S}A_{IB}{}^{(1)}\mathrm{A_{BB}^{-1}}{}^{(1)}\mathrm{A_{BI}}{}^{(1)} + yS^{-1}\dot{S}\mathrm{A_{II}}{}^{(1)}\right]\{\mathrm{W_I}\}\right)_1 \\ + (\mathrm{A_{BB}^{-1}}{}^{(1)}\Omega_{BB}[S^{-1}\mathrm{A_{IB}}{}^{(2)} + y\dot{S}\mathrm{A_{IB}}{}^{(1)}]\{Q_{\mathrm{BC}}\})_1 \\ \frac{\mathrm{d}}{\mathrm{d}\tau}\{\mathrm{W_I}\}_2 = \left([Na.(1-S)^{-2}\mathrm{A_{II}}{}^{(2)} + (1-z)(1-S)^{-1}\dot{S}\mathrm{A_{II}}{}^{(1)}]\{\mathrm{W_I}\}\right)_2 \\ + \left([Na.(1-S)^{-2}\mathrm{A_{IB}}{}^{(2)} + (1-z).(1-S)^{-1}\dot{S}\mathrm{A_{IB}}{}^{(1)}]\{\theta_{\mathrm{BC}}\}\right)_2 \\ \frac{\mathrm{d}}{\mathrm{d}\tau}\{\dot{S}\} = \Omega_B^{-1}\left(\left[\mathrm{G_{BI}}{}^{(1)}S^{-1} - S^{-1}A_{BI}{}^{(1)}G_{BB}^{(1)}A_{BB}^{-1(1)}\right]\{\mathrm{W_I}\}\right)_1 - \left([\mathrm{G_{BI}}{}^{(1)}Nk(1-S)^{-1}]\{\mathrm{W_I}\}\right)_2 \\ -([Nk(1-S)^{-1}\mathrm{G_{BB}}{}^{(1)}]\{\theta_{\mathrm{BC}}\})_2 + \left(\left[G_{BB}^{(1)}\mathrm{A_{BB}}{}^{-1(1)}\mathrm{Q_{BC}}\Omega_{BB}\right]\{Q_{\mathrm{BC}}\}\right)_1 \\ (\mathrm{A_{BB}W_B})_2 = (\theta_{\mathrm{BC}})_2, \mathrm{A_{BB}} = I \end{cases}$		

5 Convergence and validation

The exact solution of the properties reported in Table 2 is compared with GDQM. In this study, a kind of n-paraffin has been chosen for the specific purpose of the battery thermal management systems (BTMS) because of its acceptable or constant phase change temperature [41] and also having constant cooling temperature [42].

Table 2. PCM properties [43]

PCM type	**6106 (n-paraffin)**
Fusion entahlpy, kJ/kg	189
Thermal conductivity, $W/m.K$	0.21
Density(solid/liquid), kg/m^3	910/765
Specific heat, $kJ/kg.K$	2.1
Melting temperature(K)	316

5.1 Convergence and computational cost

The GDQM's specific feature is that the most precise solution is likely even with limited grid points. Sensitivity analysis investigates the effect of the number of nodes (N and M are liquid and solid phase, respectively) on the interphase position s(t). Liquid and solid phases have the same number of N and M, respectively.

Figure 3 shows an insignificant variation between the answer achieved with N=M=7 and greater values, and the response for values greater than N=M =10. Furthermore, the figure illustrates that the difference between N=M=10 and 40 is almost zero for the sum of grids in the melted part, a special feature of this approach. This figure additionally shows that the computational cost for the suggested technique is appropriately low in seconds.

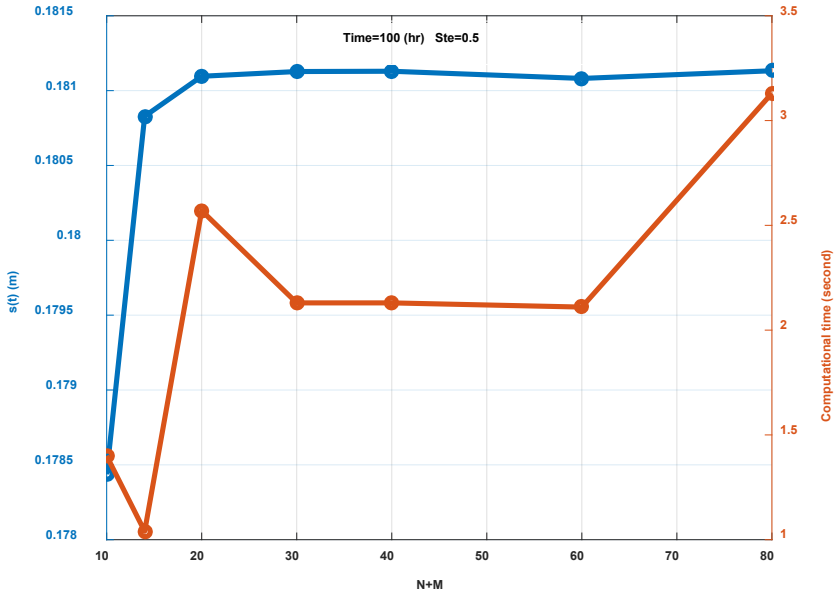

Figure 3. The convergence of GDQM reactions to Stefan's problem and its calculation cost. Interface and cost compared to node's number (N+M).

5.2 The Exact formulation

The analytical formulation for the two-phase Stefan problem is presented here [44];

$$T_1(x,t) = T_l - (T_l - T_m)\frac{\operatorname{erf}\left(\frac{x}{2.\sqrt{\alpha_1 t}}\right)}{\operatorname{erf}(\lambda)}, \qquad 0 \le x \le s(t) \tag{41}$$

$$T_2(x,t) = T_r + (T_m - T_r)\frac{\operatorname{erfc}\left(\frac{x}{2.\sqrt{\alpha_2 t}}\right)}{\operatorname{erfc}\left(\lambda\sqrt{\frac{\alpha_1}{\alpha_2}}\right)}, \qquad x \ge s(t) \tag{42}$$

Where $\lambda = \frac{S}{2\tau^{\frac{1}{2}}}$ and can be obtained from:

$$\frac{Ste_1}{\exp(\lambda^2).\operatorname{erf}(\lambda)} - \frac{Ste_2}{(\alpha_1/\alpha_2)\exp\left((\alpha_1/\alpha_2)^2\lambda^2\right).erfc((\alpha_1/\alpha_2)\lambda)} = \lambda\sqrt{\pi} \tag{43}$$

In this equation, 1 shows the liquid, and 2 shows the state of solid.

Figures 4 illustrate the temperature and error distribution's comparison between the exact analytical solution and the GDQ/heat capacity methods. Findings were computed along with four various times $t = 1,10,50,\text{and } 100(\text{hr})$. The number of Grid Points N and M for these comparisons is equal to 20. The error was calculated for the cases considered in these figures as:

$$Error(\%) = 100 * \frac{\theta_{Exact} - \theta_{GDQ}}{\theta_{GDQ}} \qquad (44)$$

From figures 4 (a)&(b), the results of the GDQ are appropriately precise. The maximum percentage error is less than 5% for temperatures in the presented GDQ solution.

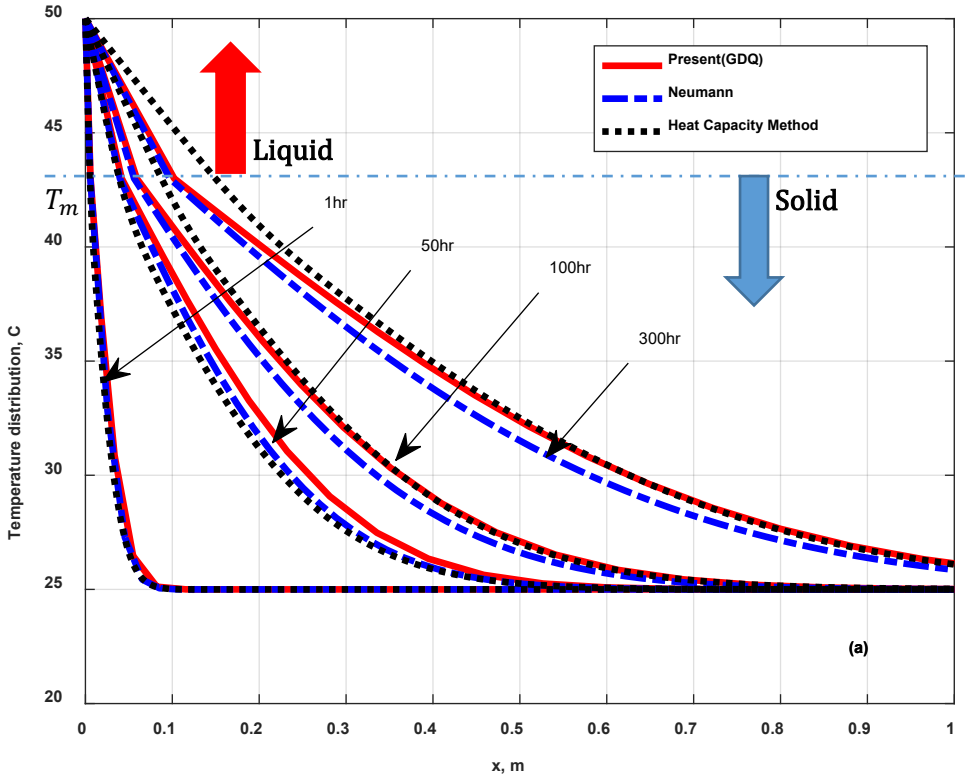

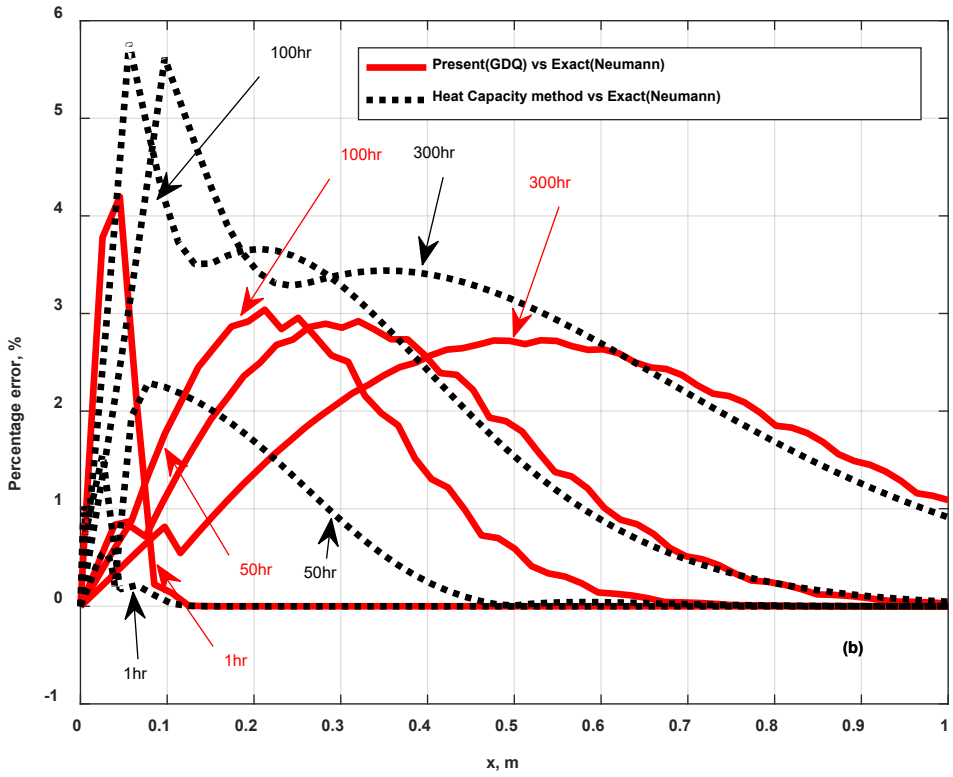

Figure 4. The temperature profile of the two-region Stefan problem was calculated by the exact, GDQM and heat capacity method (N=M=20). The temperature of the left/right side surface temperature is constant and equal to 50 and 25 °C, respectively, and the preliminary temperature of the entire slab is 25 °C. a) The distribution of temperature within the domain length. b) GDQM error results in percentage errors along the domain length.

This diagram illustrates how the GDQ method has predicted error increases and decreases over time, respectively. So, after 300 hours from the start of the process, the liquid and solid part's fluid behavior with a maximum error of 2.7% is predicted.

On the other hand, it showed that conclusions of heat capacity approach cause a larger error to the extent that this error lasted up to 6% in 100hr and 300hr. However, this error is almost two times bigger than the error of the GDQ method. The diagram shows that at longer times the results of the GDQ method are much more accurate than the heat capacity method.

Stefan number is the most critical component for precision of GDQM. Stefan numbers are typically lower than 0.2 for a latent heat thermal energy storage system (LHTS) [45]. Consequently, error analysis for Stefan numbers less than 0.2 is made in this section.

5.3 Stefan Number dependence of the error

Since the temperature at the beginning and end of the domain are involved in the calculations, to explore the impact of the Stefan number on the error, two Stefan numbers are defined in this problem, one for the hot wall temperature (left wall) and the other is for the cold wall (Right wall). For this purpose, the cold wall temperature is kept constant, and on the opposite side, the hot wall temperature and consequently the Stefan number changes. The cold wall temperature is assumed to create the Stefan number 0.2 (Stefan number usually occurs in latent energy storage problems), and the hot wall temperature changes between the temperature 50℃ (Ste.l = 0.078) and 70℃ (Ste.l = 0.3).

Figure 5 (a) illustrates the temperature distribution of the solid and liquid zones obtained by the exact solution and GDQM after 100 hours. Also, the location of the interface during 100 hours is shown in Fig. 5 (c). The error rate of the temperature profile and the interface location in the GDQ method compared to the exact solution is shown in Fig. 5 (b) and Figs. 5 (d).

The error is directly proportional to the Stefan number. The solution yields less than 4.5 % errors for Stefan numbers up to 0.2, as could be observed in Fig. 5(b). The error resulting from the interface location also shows that the GDQ method predicts the interface location with more errors by increasing the Stefan number. However, this error decreases over time. As can be seen for Stephen 0.2, the error is initially 7.6%, which reduces to approximately 7.3% after 100 hours.

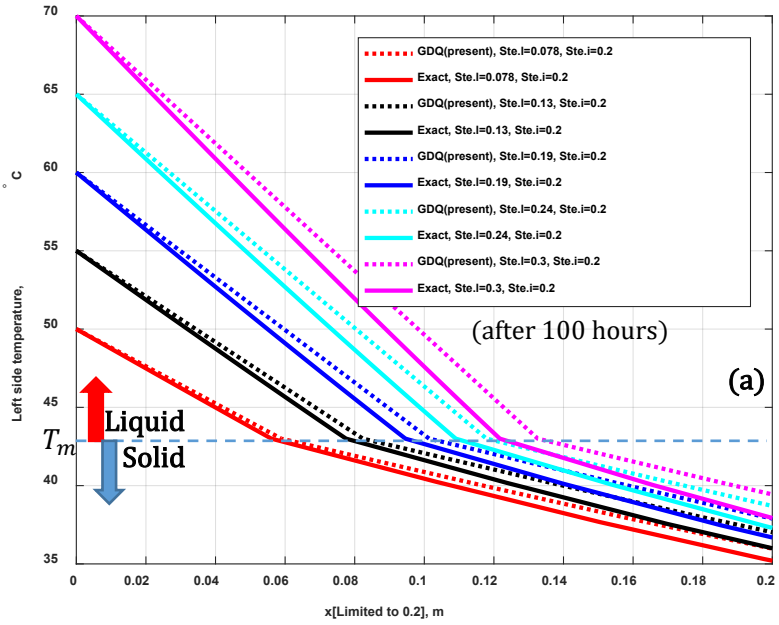
GDQ(present), Ste.l=0.078, Ste.i=0.2
Exact, Ste.l=0.078, Ste.i=0.2
GDQ(present), Ste.l=0.13, Ste.i=0.2
Exact, Ste.l=0.13, Ste.i=0.2
GDQ(present), Ste.l=0.19, Ste.i=0.2
Exact, Ste.l=0.19, Ste.i=0.2
GDQ(present), Ste.l=0.24, Ste.i=0.2
Exact, Ste.l=0.24, Ste.i=0.2
GDQ(present), Ste.l=0.3, Ste.i=0.2
Exact, Ste.l=0.3, Ste.i=0.2
(after 100 hours)
(a)
Liquid
Solid
T_m
° C
Left side temperature,
x[Limited to 0.2], m

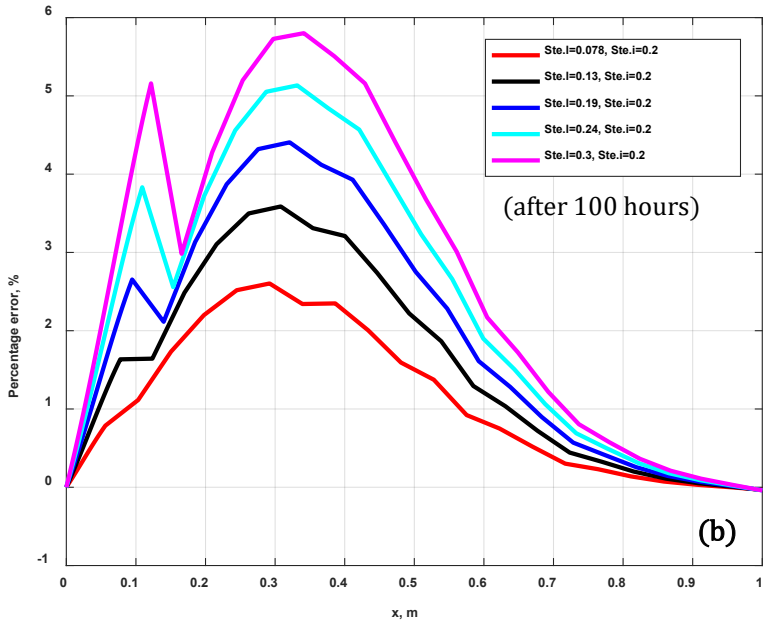
Ste.l=0.078, Ste.i=0.2
Ste.l=0.13, Ste.i=0.2
Ste.l=0.19, Ste.i=0.2
Ste.l=0.24, Ste.i=0.2
Ste.l=0.3, Ste.i=0.2
(after 100 hours)
(b)
Percentage error, %
x, m

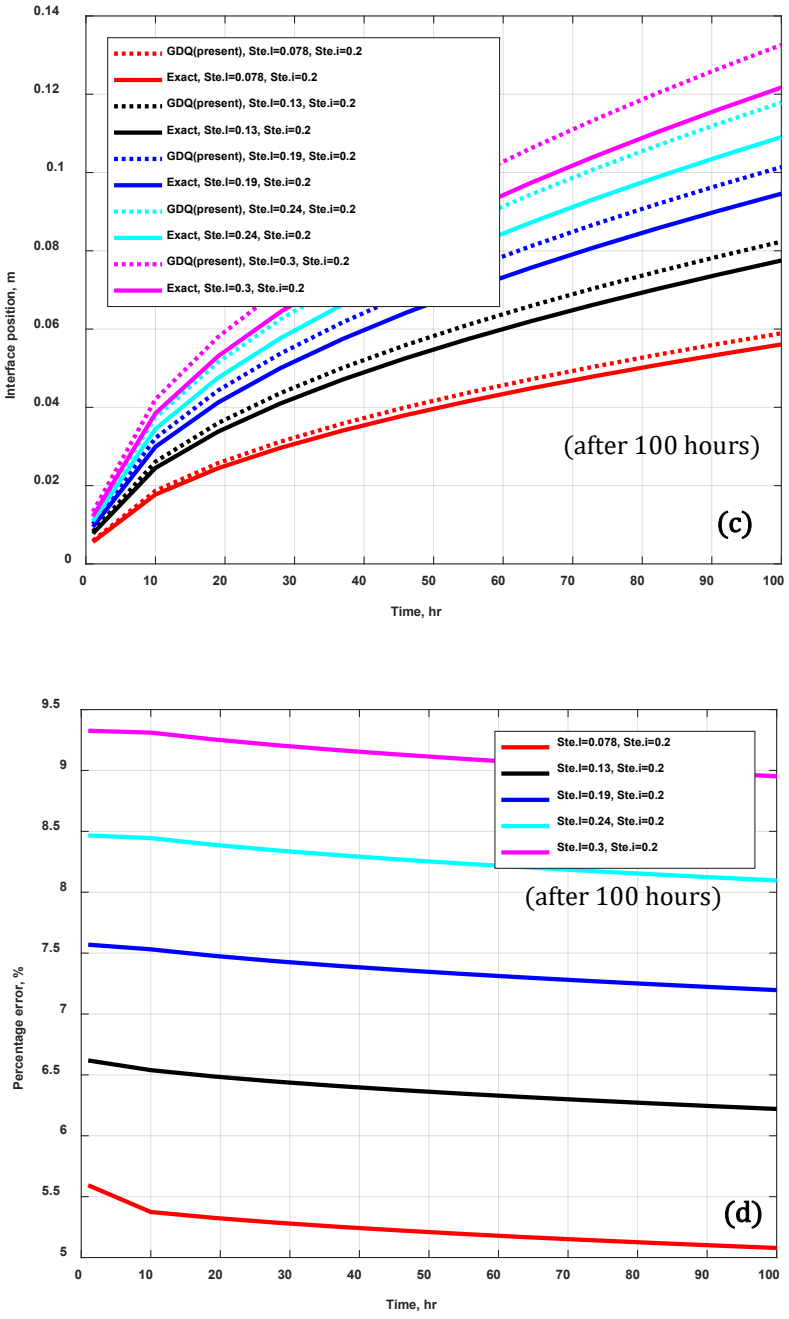

Figure 5. (a) The temperature profile of the slab, and (d) the effect of various Stefan numbers on interface position solved by the exact solution and GDQM. (b & d) The error of the GDQM concerning distinct Stefan numbers

6 Conclusion

Differential equations were achieved and normalized into a non-dimensionalized form of the one-dimensional two-region Stefan problem. The problem's specific

equations were accomplished and mathematically solved with the generalized differential quadrature method (GDQM).

In the previous article [37], we introduced this method for phase change problems only in one phase. Then in another article [36], we used it practically and evaluated various materials that can be used as PCM in thermal management systems. Here in this article, the previously existing restriction (restriction of use in one phase) is removed. Now, the behavior of PCMs can be studied in two phases with more diverse boundary conditions. Convergence and comparisons show that the proposed method for latent heat energy storage systems is sufficiently reliable (LHTS). This method can solve problems that conventional numerical or analytical methods cannot solve. Simulation of some boundary conditions and complex geometries is impossible in the analytical method, and numerical methods often do not have sufficient accuracy and speed in solving problems. For instance, simulation of multilayered PCM composite fibers (Electrospun PCM fibers) stacked on top of each other is challenging due to having a large number of very thin micron composite layers. Nevertheless, by using this method, the behavior of these composites can be easily, quickly, and accurately predicted.

However, the major problem is introducing a reformulated type of multiphase problem, which a semi-analytical method called GDQM could solve based on the performed analyses.

By inspecting the precision of the proposed LHTS problem using the GDQ approach, it was shown that;

- The GDQ method has much less error compared to the heat capacity method at longer processing times.
- The specific aspect of the GDQM is that it could result in the most precise answers even within a few grid points.

- The maximum error in the presented GDQ solution for all Stefan numbers up to 0.3 is less than 6 % for temperatures and 9.5% for interface position. The most significant factor in the precision of GDQM is the Stefan number.
- Stefan's number directly affects the error. By enhancing the surface temperature (T_l) of the left side, the Stefan number had been changing. For $Ste \leq 0.2$, GDQ's errors are $\leq 4.2\%$ for temperature and $\leq 7.5\%$ for interface location, and subsequently, the suggested attitude is favorable for this usage.
- As the processing time increases, the GDQ method predicts the temperature profile and interface position with less error.

This model can present a suitable outline for simulating and modeling other practical settings for upcoming work in the perception of the complete validation of the model presented.

Information accessibility statement

The full information will be accessible upon request.

References

[1] V. Voller and M. Cross, "Accurate solutions of moving boundary problems using the enthalpy method," *International Journal of Heat and Mass Transfer,* vol. 24, no. 3, pp. 545-556, 1981/03/01/ 1981, doi: https://doi.org/10.1016/0017-9310(81)90062-4.

[2] M. Yao and A. Chait, "AN ALTERNATIVE FORMULATION OF THE APPARENT HEAT CAPACITY METHOD FOR PHASE-CHANGE PROBLEMS," *Numerical Heat Transfer, Part B: Fundamentals,* vol. 24, no. 3, pp. 279-300, 1993/10/01 1993, doi: 10.1080/10407799308955894.

[3] J. Mennig and M. Özişik, "Coupled integral equation approach for solving melting or solidification," *International journal of heat and mass transfer,* vol. 28, no. 8, pp. 1481-1485, 1985.

[4] R. Kothari, S. Das, S. K. Sahu, and S. I. Kundalwal, "Analysis of solidification in a finite PCM storage with internal fins by employing heat balance integral method," *International Journal of Energy Research,* vol. 0, no. 0, doi: 10.1002/er.4363.

[5] M. Alizadeh, K. Hosseinzadeh, and D. Ganji, "Investigating the effects of hybrid nanoparticles on solid-liquid phase change process in a Y-shaped fin-assisted LHTESS by means of FEM," *Journal of Molecular Liquids,* vol. 287, p. 110931, 2019.

[6] M. Alizadeh, K. Hosseinzadeh, H. Mehrzadi, and D. Ganji, "Investigation of LHTESS filled by Hybrid nano-enhanced PCM with Koch snowflake fractal cross section in the presence of thermal radiation," *Journal of Molecular Liquids,* vol. 273, pp. 414-424, 2019.

[7] K. Hosseinzadeh, M. Alizadeh, M. Alipour, B. Jafari, and D. Ganji, "Effect of nanoparticle shape factor and snowflake crystal structure on discharging acceleration LHTESS containing (Al2O3-GO) HNEPCM," *Journal of Molecular Liquids,* p. 111140, 2019.

[8] M. Safdari, R. Ahmadi, and S. Sadeghzadeh, "Numerical investigation on PCM encapsulation shape used in the passive-active battery thermal management," *Energy,* vol. 193, p. 116840, 2020/02/15/ 2020, doi: https://doi.org/10.1016/j.energy.2019.116840.

[9] J. Lee and K.-Y. Hwang, "A hybrid numerical analysis of heat transfer and thermal stress in a solidifying body using FVM and FEM," *International journal of engineering science,* vol. 34, no. 8, pp. 901-922, 1996.

[10] C. W. Bert and M. Malik, "FREE VIBRATION ANALYSIS OF TAPERED RECTANGULAR PLATES BY DIFFERENTIAL QUADRATURE METHOD: A SEMI-ANALYTICAL APPROACH," *Journal of Sound and Vibration,* vol. 190, no. 1, pp. 41-63, 1996/02/15/ 1996, doi: https://doi.org/10.1006/jsvi.1996.0046.

[11] R. Bellman and J. Casti, "Differential quadrature and long-term integration," *Journal of Mathematical Analysis and Applications,* vol. 34, no. 2, pp. 235-238, 1971.

[12] R. Bellman, B. Kashef, and J. Casti, "Differential quadrature: a technique for the rapid solution of nonlinear partial differential equations," *Journal of computational physics,* vol. 10, no. 1, pp. 40-52, 1972.

[13] C. Shu and B. E. Richards, "Application of generalized differential quadrature to solve two-dimensional incompressible Navier-Stokes equations," *International Journal for Numerical Methods in Fluids,* vol. 15, no. 7, pp. 791-798, 1992.

[14] C. Shu and B. Richards, "High resolution of natural convection in a square cavity by generalized differential quadrature," in *Proceedings of the 3rd International Conference on Advances in Numeric Methods in Engineering: Theory and Application, Swansea, UK*, 1990, pp. 978-985.

[15] J.-a. Sun and Z.-y. Zhu, "Upwind local differential quadrature method for solving incompressible viscous flow," *Computer Methods in Applied Mechanics and Engineering,* vol. 188, no. 1, pp. 495-504, 2000/07/21/ 2000, doi: https://doi.org/10.1016/S0045-7825(99)00191-7.

[16] B. Kashef and R. Bellman, "Solution of the partial differential equation of the Hodgkin-Huxley model using differential quadrature," *Mathematical Biosciences,* vol. 19, no. 1-2, pp. 1-8, 1974.

[17] J. O. Mingle, "The method of differential quadrature for transient nonlinear diffusion," *Journal of Mathematical Analysis and Applications,* vol. 60, no. 3, pp. 559-569, 1977.

[18] G. Naadimuthu, R. Bellman, K. Wang, and E. Lee, "Differential quadrature and partial differential equations: some numerical results," *Journal of mathematical analysis and applications,* vol. 98, no. 1, pp. 220-235, 1984.

[19] F. Civan and C. Sliepcevich, "Application of differential quadrature to transport processes," *Journal of Mathematical Analysis and Applications,* vol. 93, no. 1, pp. 206-221, 1983.

[20] F. Civan and C. Sliepcevich, "Solution of the Poisson equation by differential quadrature," *International journal for numerical methods in engineering,* vol. 19, no. 5, pp. 711-724, 1983.

[21] C. BERT, S. JANG, and A. STRIZ, "New methods for analyzing vibration of structural components," in *28th Structures, Structural Dynamics and Materials Conference*, 1987, p. 950.

[22] R. Saini and R. Lal, "Effect of Thermal Environment and Peripheral Loading on Axisymmetric Vibrations of Non-uniform FG Circular Plates via Generalized Differential Quadrature Method," *Journal of Vibration Engineering & Technologies,* 2021/01/18 2021, doi: 10.1007/s42417-020-00270-x.

[23] M. Javani, Y. Kiani, and M. R. Eslami, "Application of generalized differential quadrature element method to free vibration of FG-GPLRC T-shaped plates," *Engineering Structures,* vol. 242, p. 112510, 2021.

[24] M. Korayem, A. Karimi, and S. Sadeghzadeh, "GDQEM analysis for free vibration of V-shaped atomic force microscope cantilevers," *International Journal of Nanoscience and Nanotechnology,* vol. 10, no. 4, pp. 205-214, 2014.

[25] H. Edalati, V. Daghigh, and K. Nikbin, "Critical buckling load of composite laminates containing delamination using differential quadrature method and ABAQUS finite element," *The Journal of Strain Analysis for Engineering Design,* p. 0309324721996579, 2021.

[26] T. Thumma, A. Wakif, and I. L. Animasaun, "Generalized differential quadrature analysis of unsteady three-dimensional MHD radiating dissipative Casson fluid conveying tiny particles," *Heat Transfer,* vol. 49, no. 5, pp. 2595-2626, 2020.

[27] M. U. Ashraf, M. Qasim, A. Wakif, M. I. Afridi, and I. L. Animasaun, "A generalized differential quadrature algorithm for simulating magnetohydrodynamic peristaltic flow of blood-based nanofluid containing magnetite nanoparticles: a physiological application," *Numerical Methods for Partial Differential Equations,* 2020.

[28] M. S. Hashmi, M. Wajiha, S.-W. Yao, A. Ghaffar, and M. Inc, "Cubic Spline Based Differential Quadrature Method: A Numerical Approach for Fractional Burger Equation," *Results in Physics,* p. 104415, 2021.

[29] A. Mokhalingam, D. Kumar, and A. Srivastava, "Mechanical Behaviour of Graphene Reinforced Aluminum Nano composites," *Materials Today: Proceedings,* vol. 4, no. 2, pp. 3952-3958, 2017.

[30] H. Hao and D. Lau, "Atomistic modeling of metallic thin films by modified embedded atom method," *Appl. Surf. Sci.,* vol. 422, pp. 1139-1146, 2017.

[31] C. Shu, B. C. Khoo, K. S. Yeo, and Y. T. Chew, "Application of GDQ scheme to simulate natural convection in a square cavity," *International Communications in Heat and Mass Transfer,* vol. 21, no. 6, pp. 809-817, 1994/11/01/ 1994, doi: https://doi.org/10.1016/0735-1933(94)90034-5.

[32] M.-I. Char, F.-P. Chang, and B.-C. Tai, "Inverse determination of thermal conductivity by differential quadrature method," *International Communications in Heat and Mass Transfer,* vol. 35, no. 2, pp. 113-119, 2008/02/01/ 2008, doi: https://doi.org/10.1016/j.icheatmasstransfer.2007.06.006.

[33] T. S., "DQ-based simulation of weakly nonlinear heat conduction processes," *Communications in Numerical Methods in Engineering,* vol. 24, no. 11, pp. 1523-1532, 2008, doi: doi:10.1002/cnm.1049.

[34] G. Meral, "Differential quadrature solution of heat- and mass-transfer equations," *Applied Mathematical Modelling,* vol. 37, no. 6, pp. 4350-4359, 2013/03/15/ 2013, doi: https://doi.org/10.1016/j.apm.2012.09.012.

[35] P. Malekzadeh, H. Rahideh, and G. Karami, "A differential quadrature element method for nonlinear transient heat transfer analysis of extended surfaces," *Numerical Heat Transfer, Part A: Applications,* vol. 49, no. 5, pp. 511-523, 2006.

[36] M. Safdari, S. Sadeghzadeh, and R. Ahmadi, "Tailoring the life cycle of lithium-ion batteries with a passive cooling system: A comprehensive dynamic model," *International Journal of Energy Research,* vol. 45, no. 5, pp. 7884-7902, 2021, doi: https://doi.org/10.1002/er.6373.

[37] M. Safdari, S. Sadeghzadeh, and R. Ahmadi, "A semi-analytical solution for time-varying latent heat thermal energy storage problems," *International Journal of Energy Research,* vol. 44, no. 4, pp. 2726-2739, 2020, doi: https://doi.org/10.1002/er.5078.

[38] A. Faghri and Y. Zhang, *Transport phenomena in multiphase systems*. Elsevier, 2006.
[39] C. Huber, "Phase Change Material in Battery Thermal Management Applications," Technische Universität München, 2017.
[40] M. Janghorban, "Two different types of differential quadrature methods for static analysis of microbeams based on nonlocal thermal elasticity theory in thermal environment," *Archive of Applied Mechanics,* vol. 82, no. 5, pp. 669-675, 2012.
[41] A. Abhat, "Low temperature latent heat thermal energy storage: heat storage materials," *Solar energy,* vol. 30, no. 4, pp. 313-332, 1983.
[42] T. R. Dennis K. Phase change materials & heat pump analysis for an electric vehicle. Department of Mechanical Engineering, Lakehead University 1995.
[43] Z. Rao and S. Wang, "A review of power battery thermal energy management," *Renewable and Sustainable Energy Reviews,* vol. 15, no. 9, pp. 4554-4571, 2011.
[44] V. Alexiades and A. D. Solomon, "Mathematical modeling of melting and freezing processes, Hemisphere Publ," *Corp., Washington,* 1993.
[45] C. Shu, *Differential Quadrature and Its Application in Engineering*. Springer London, 2012.